

IEEE/NSS Toronto,
Nov. 9, 1998

Single photon detection

Peter Križan

*University of Ljubljana and J. Stefan Institute,
Ljubljana, Slovenia*

- Introduction
- Photosensitive materials
- Detection of single electrons
- Feed-back photons
- High rate operation, ageing
- Chambers for detection of UV, visual photons
- Ring Imaging Čerenkov counters
- Other applications

Motivation

Photomultiplier tubes are meant for detection of light.

Why bother to develop light sensitive chambers?

Well,

- some applications need good spatial resolution (order few mm),
- some applications require coverage of large surfaces (square meters) with a large fraction of active area at reasonable cost,
- some applications need a highly efficient single photon detection,
- some applications require all of it.

Introduction

Wire chambers detect **charged particles**. To detect a **photon**, one has to make sure it reacts with the chamber material, walls or gas, and produces a photoelectron, which is then detected in the chamber.

A well known example: detection of **X-rays** in a MWPC with an argon-methane gas mixture.

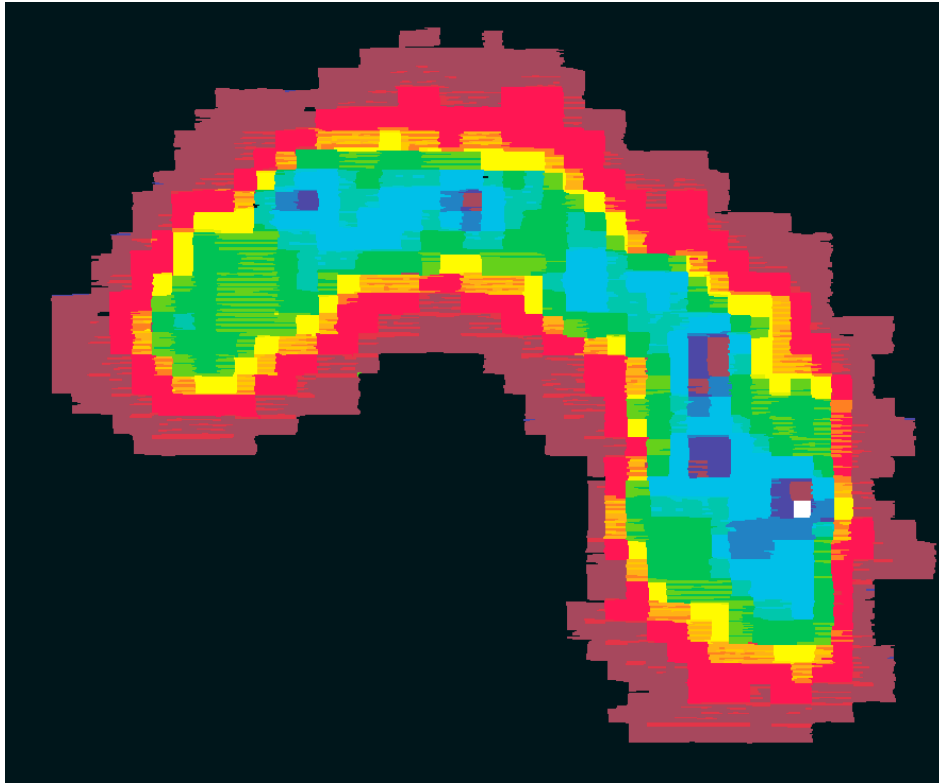
Can one detect **UV** or **visual** photons as well?

In principle yes, however

- a photosensitive material is needed that survives in the chamber gas mixture (PMTs have vacuum inside!)
- the photoelectron produced has a very low energy, so that it does not make any more primary electron-ion pairs - the avalanche is started by a single electron.

Example: metal surface

Note that any metal surface, in particular if polished, is sensitive to visual light, although with a very low efficiency.



The photograph of the tungsten filament in a light bulb was taken with a small 5cm x 5cm MWPC with a two dimensional delay line read-out, the object was projected onto the cathode plane through a small hole in a black box (*camera obscura*). From: M. Starič et al., NIM **A323** (1992) 91-96

Photosensitive materials

To get a reasonable efficiency, order 10%-20%, one has to use quite special materials.

They are typically chemically active, so that care has to be taken on how they are handled, and how clean the inside of the chamber is.

- Photosensitive gas additives

TEA Tri Ethyl Amine

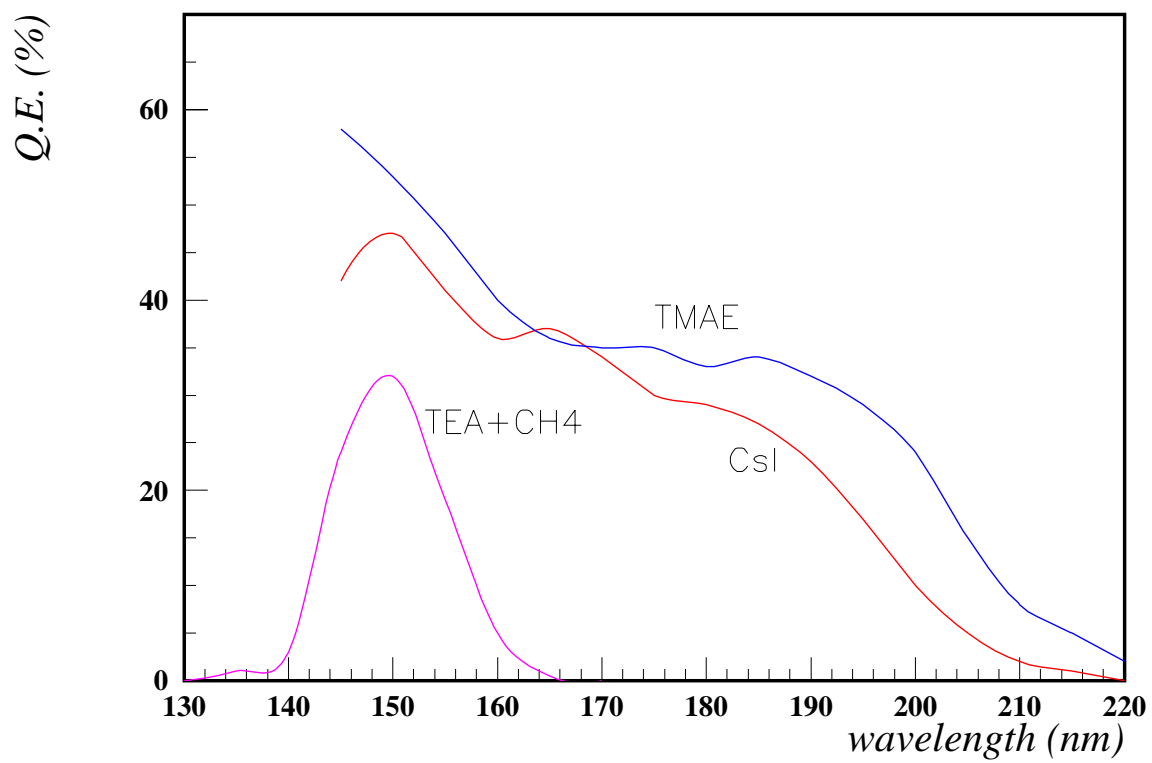
TMAE Tetrakis diMethyl Amino Ethylene

- Solid photosensitive layers on the read-out cathode or entrance window

CsI

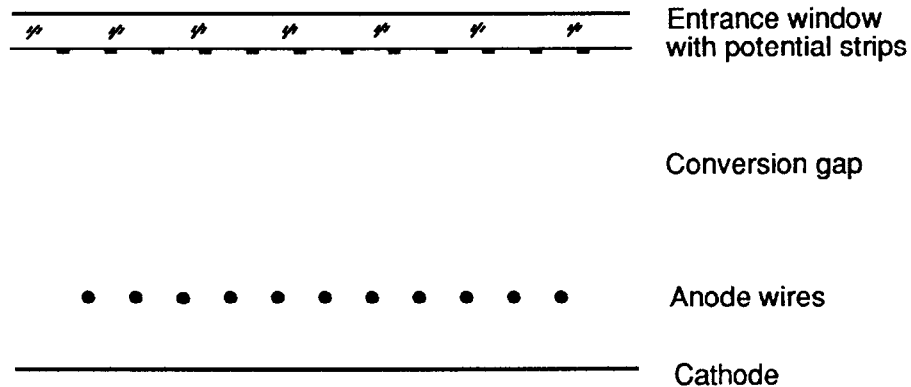
new materials e.g. K-Cs-Sb, coated with CsBr or

CsI: sensitive in visual, still under study



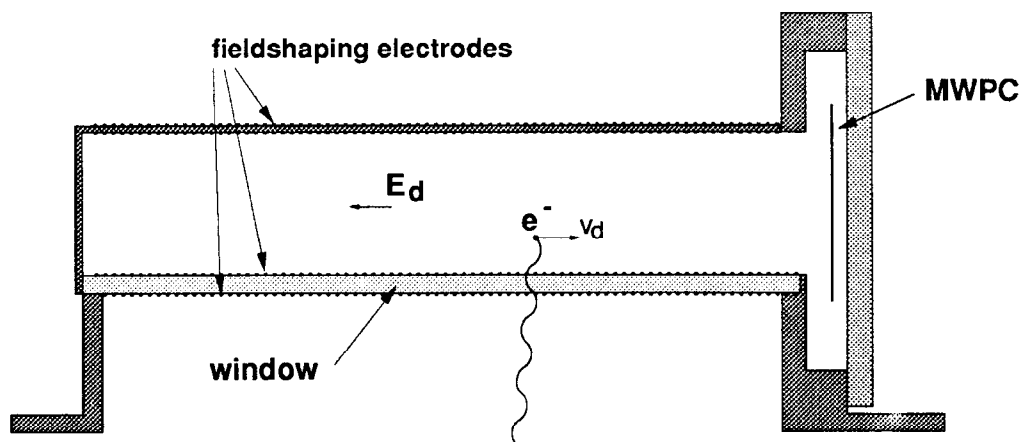
TEA

- A liquid at room temperature, with a vapour pressure of 52 torr (at 20⁰C) and the absorption cross section $\sigma_{UV} = 10Mb$.
- Absorption length of 0.61mm (at 20⁰C).
- Typical chamber: a multiwire chamber with pad read-out.



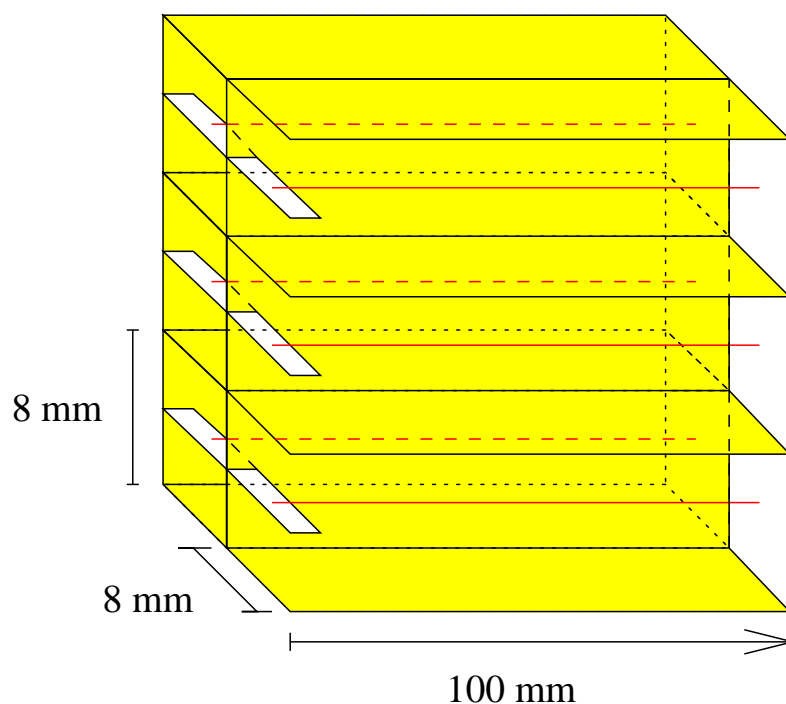
TMAE

- A liquid at room temperature, with a vapour pressure of 0.30 torr (at 20⁰C) and the absorption cross section $\sigma_{UV} = 30Mb$.
- Absorption length of about 3 cm at room temperature.
- Typical chamber: a thick conversion volume is needed to enable an efficient absorption, usually combined with a TPC type chamber.



- Gas purity: very clean system needed (TMAE reacts intensely with oxygen!), stainless steel pipes and valves, oxysorb.

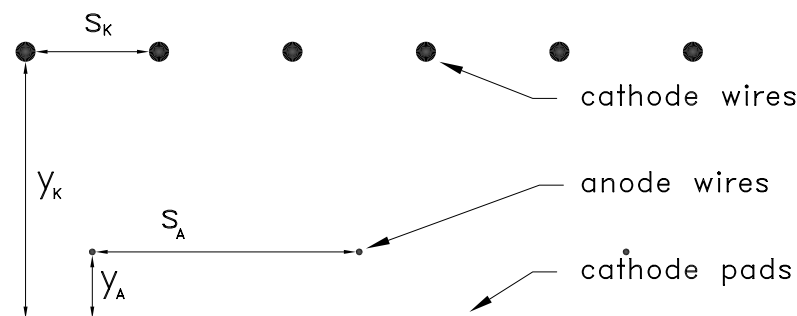
- Chamber materials: TMAE reacts with most common chamber materials.
- Higher rates: a different geometry is needed. An example is the JETSET/HERA-B prototype geometry with anode wires embedded in an egg-crate structure.



Photons enter the chamber from the left side.



- A solid layer, 100nm - 1 μ m thick, evaporated on one of the cathodes (or on the entrance window).
- Needs a high purity chamber gas, usually methane with a water and oxygen content of order ppm.
- Typical chamber: a multiwire chamber with pad read-out, reflective photocathode.

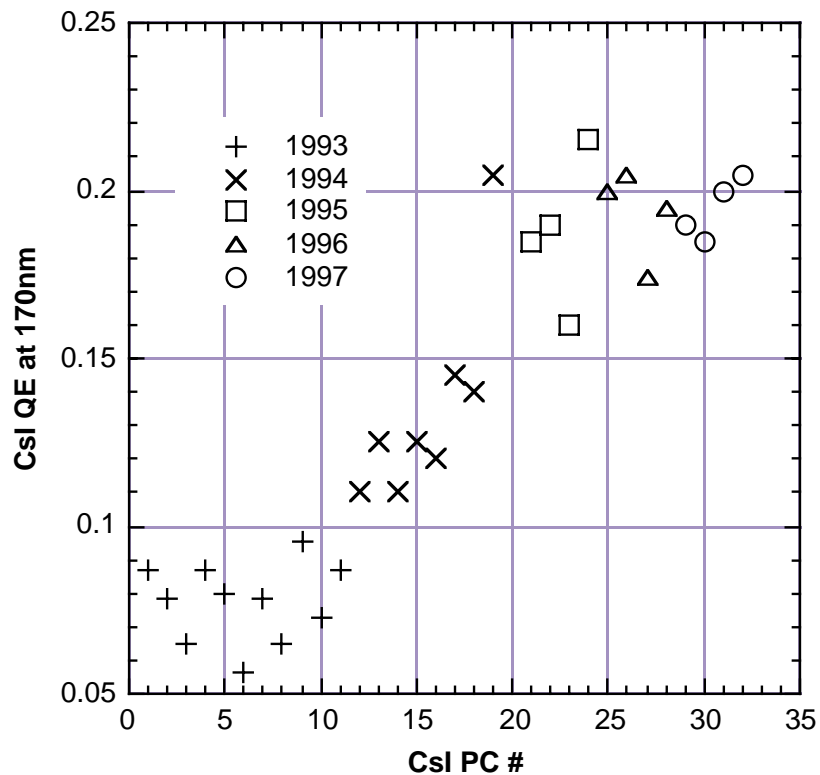


- Electric field: voltage on cathode wires has to be adjusted to guarantee a uniform amplification around the anode wire.
- Chamber variation: photocathode evaporated on the entry window, chamber can then be a MSGC, MGC, can also have a GEM amplification structure and multiwire chamber with pad read-out.

CsI cathode handling

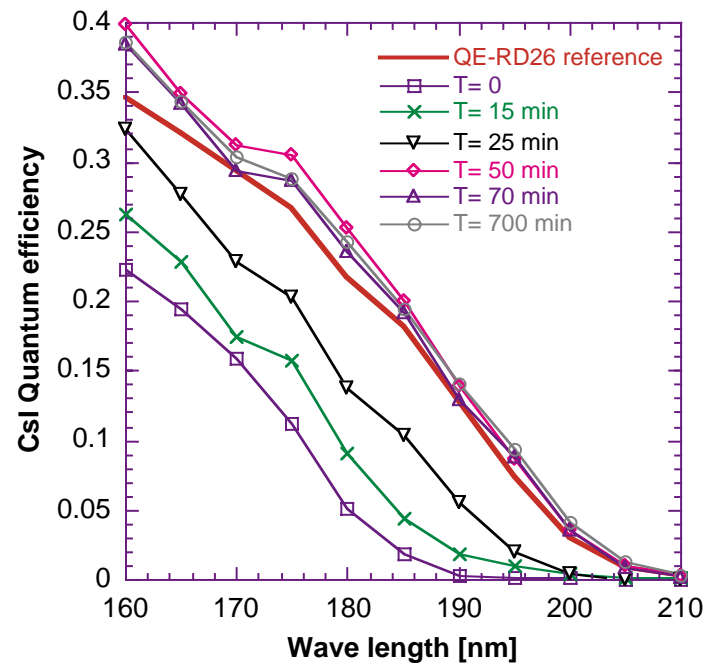
A lot of progress in R+D over the past few years:

□ learning curve: Q.E. vs. t, RD-26



□ influence of substrate material (-> photo)

- influence of initial conditioning: keeping for several hours at 60 C in vacuum



- exposure to air: should not exceed 1/2 hour

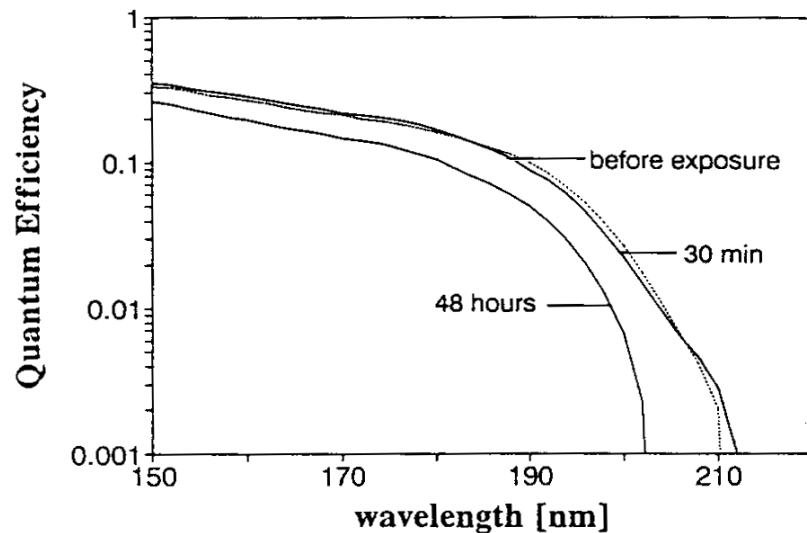
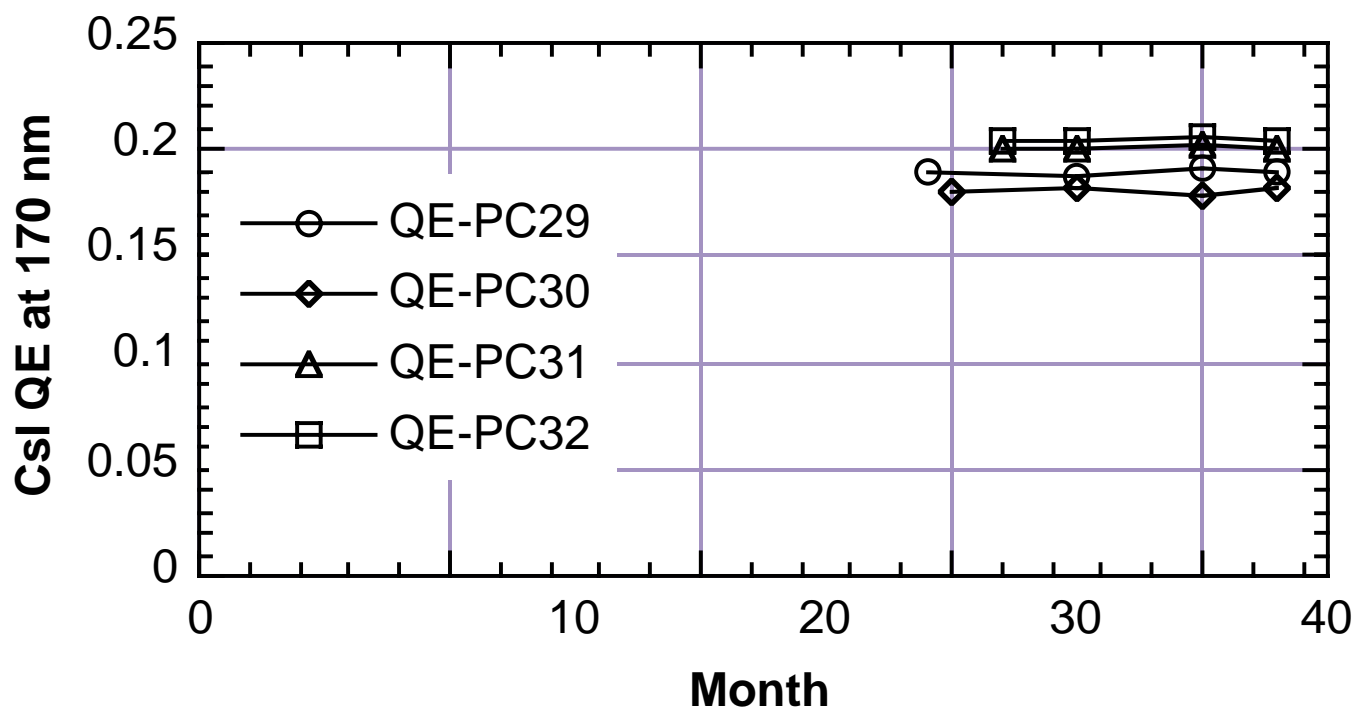
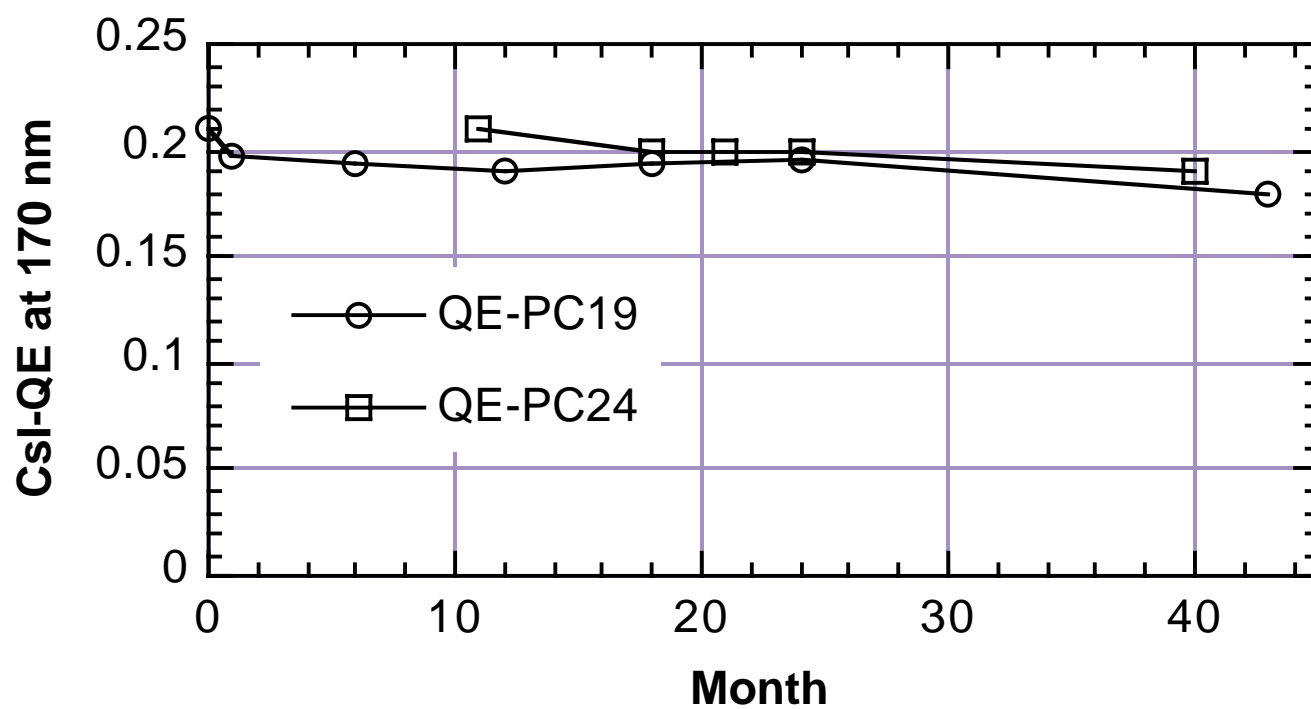


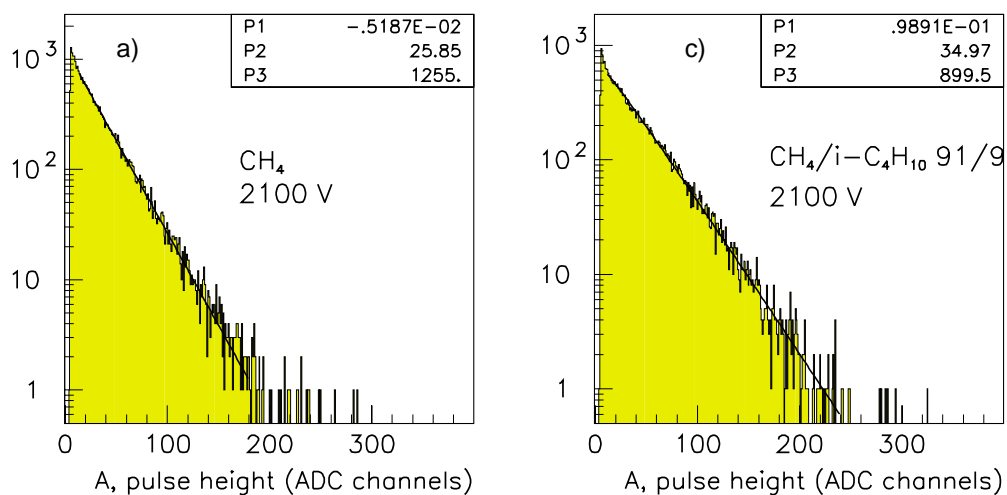
Figure 2.9: The decay of the QE of CsI layers evaporated on Ni/Au coated PCB under exposure to air at a relative humidity of 35% [6].

□ stability in the chamber



Single primary electron pulse height

A typical pulse height spectrum of single electrons has the exponential shape with a large fraction of low pulses.

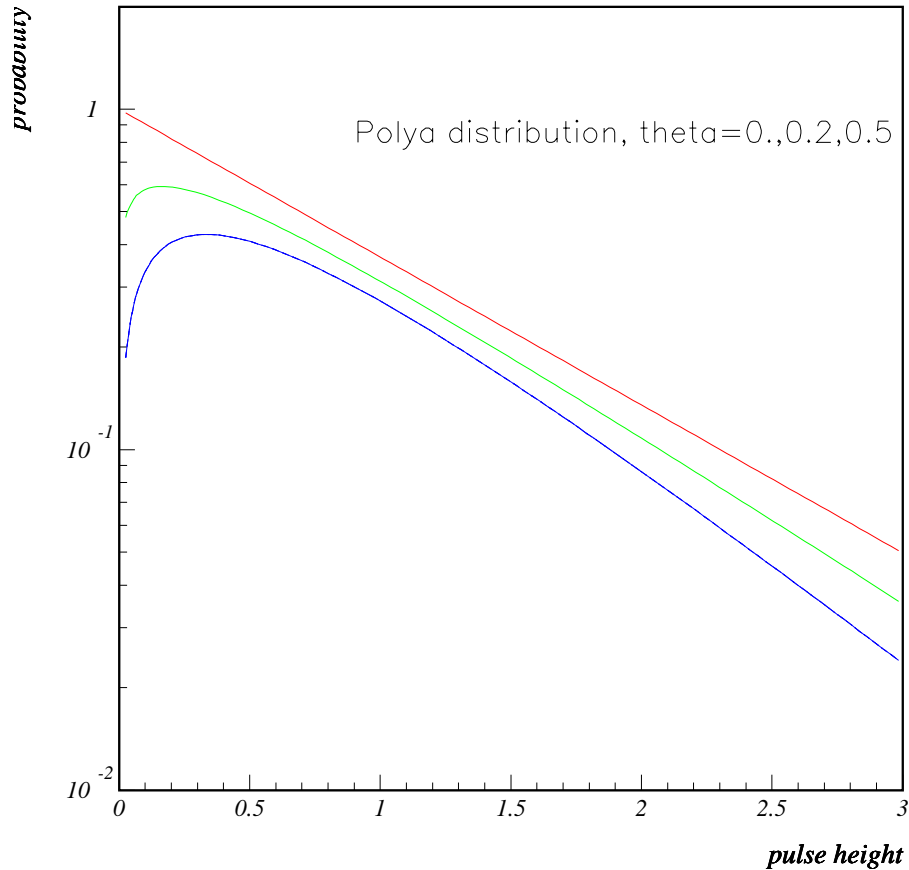


Only at high gains ($> 10^5$) the distribution flattens off at low gain, or even peaks at a nonzero value.

Data support a parametrisation of the Polya form

$$\frac{dw}{dU} = \frac{1 + \theta}{\bar{U}\Gamma(1 + \theta)} \left((1 + \theta) \frac{U}{\bar{U}} \right)^\theta e^{-(1+\theta)\frac{U}{\bar{U}}},$$

with θ ranging from 0 (exponential) to about 0.5



Statistics of the avalanche caused by a single primary electron

Avalanche multiplication is described by the multiplication coefficient α (also first Townsend coefficient). The mean free path between ionizing collisions is $1/\alpha$, and for a case of constant field on average $e^{\alpha x}$ electrons are produced in an avalanche over a distance x .

The fluctuations are, however, large, in particular due to fluctuations in the number of ionisations in the initial part of the avalanche.

The distribution over the number of electrons produced in the avalanche is derived as follows.

The probability that an electron ionizes an atom to produce a new electron is equal to

$$\alpha dx$$

Starting with one electron we ask what is the probability $P(n, x)$ that n electrons will result at a distance x ?

The probabilities have to satisfy a set of differential equations

$$\frac{d}{dx}P(1, x) = -\alpha P(1, x)$$

$$\frac{d}{dx}P(2, x) = -2\alpha P(2, x) + \alpha P(1, x)$$

.....

$$\frac{d}{dx}P(n, x) = -n\alpha P(n, x) + (n-1)\alpha P(n-1, x)$$

with the boundary conditions that we had a single electron at the beginning, $P(1, 0) = 1$; $P(n, 0) = 0, n > 1$.

By successive integration we get

$$P(1, x) = e^{-\alpha x}$$

$$P(2, x) = e^{-\alpha x} (1 - e^{-\alpha x})$$

.....

$$P(n, x) = e^{-\alpha x} (1 - e^{-\alpha x})^{n-1}.$$

Taking into account that $e^{\alpha x}$ is the mean value of n , \bar{n} , we get

$$P(n, x) = \frac{1}{\bar{n}} \left(1 - \frac{1}{\bar{n}}\right)^{n-1}.$$

which is for $n \gg 1$

$$P(n, x) = \frac{1}{\bar{n}} e^{-\frac{n}{\bar{n}}}.$$

Single primary electron detection

For the exponential pulse height distribution,

$$\frac{dw}{dU} = \frac{1}{\bar{U}} e^{-U/\bar{U}},$$

the single electron detection efficiency amounts to

$$\epsilon = \int_{U_{th}}^{\infty} \frac{dw}{dU} dU = e^{-U_{th}/\bar{U}}$$

for the pulse height threshold set to U_{th} .

For a highly efficient photoelectron detector we clearly need low noise electronics.

How low is low? The **visual charge** (see Sauli's talk) is about **20%** (for integration times of order 20ns) of the avalanche charge, i.e. at a gas amplification of **$2 \cdot 10^5$** the average detected signal corresponds to **$4 \cdot 10^4$** electrons. If we want to cut noise at **4σ** , and keep a **90%** efficiency ($U_{th} = 0.1\bar{U}$), the electronics noise has to be kept at

$$\frac{2 \cdot 10^5 \cdot 0.2 \cdot 0.1}{4} = 1000 e^- ENC$$

Photon detector problems

feedback photons

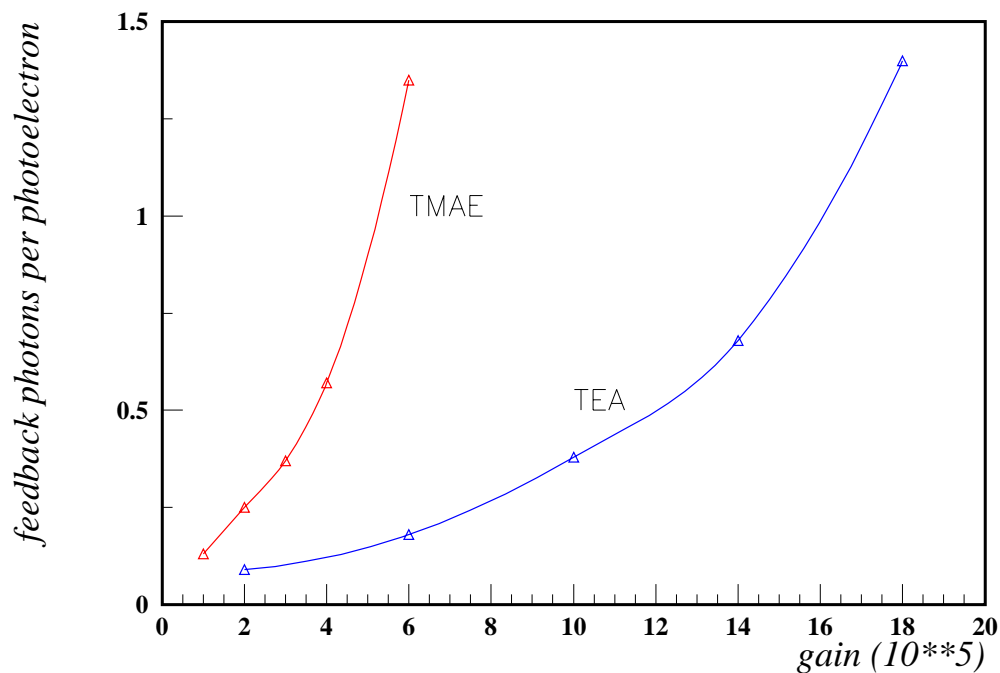
anode related effects

cathode related effects

Feedback photons

Avalanche photons cause emission of secondary photons (feedback photons). The process is enhanced because

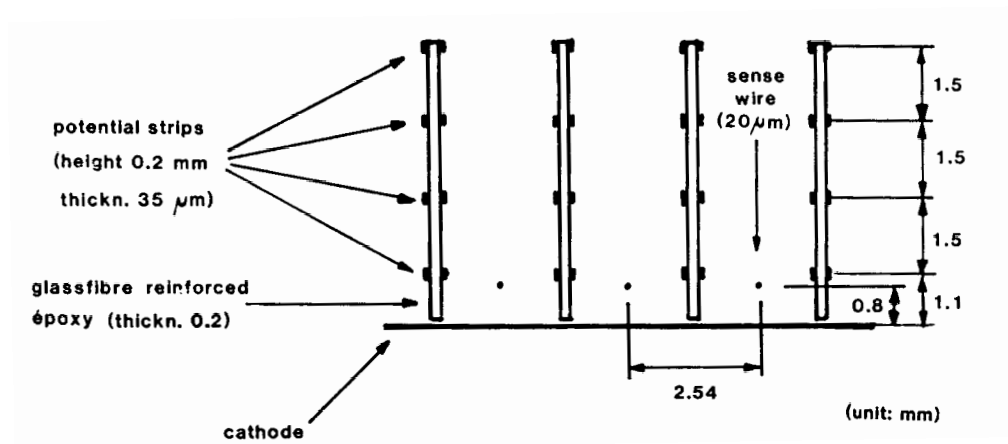
- chamber is light sensitive
- no or little quenching gas is used



The result is more background (best case) or chamber instability (in particular in cases when a lot of primary electrons are liberated by a charged track which passed the chamber).

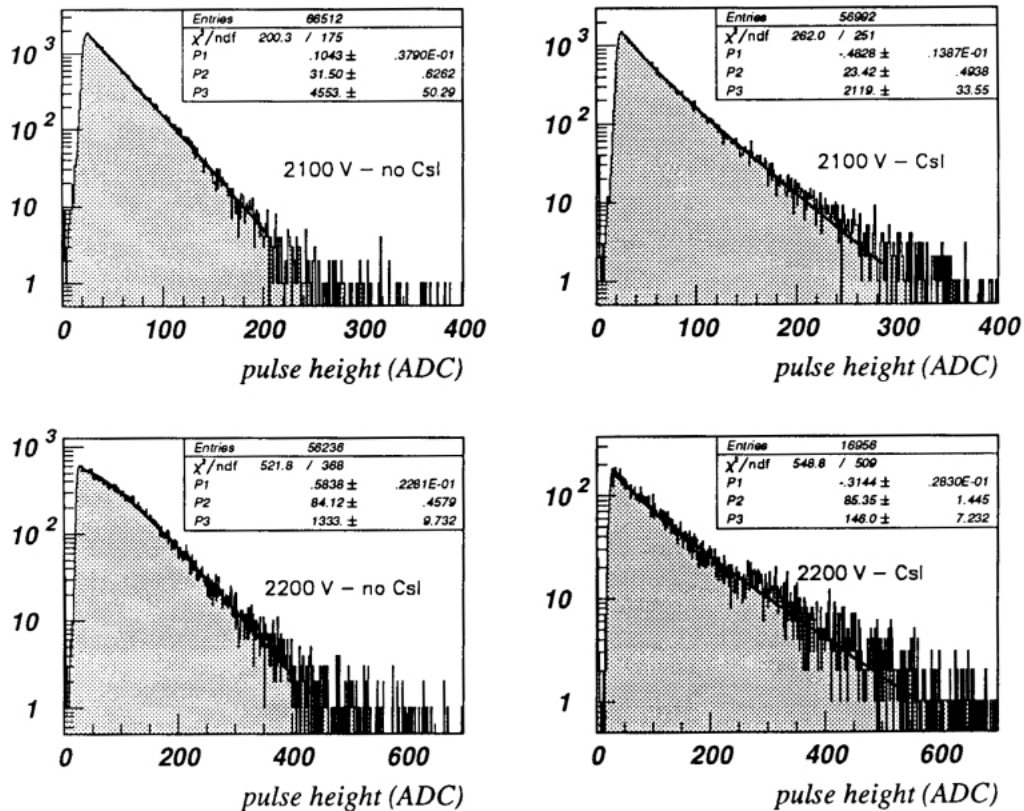
Solution:

- use isolated cell geometry a la JETSET (see above)
or
- isolate anode wires from each other by using blinds,
or



- work at low gain, preferably in a region with no charged tracks.

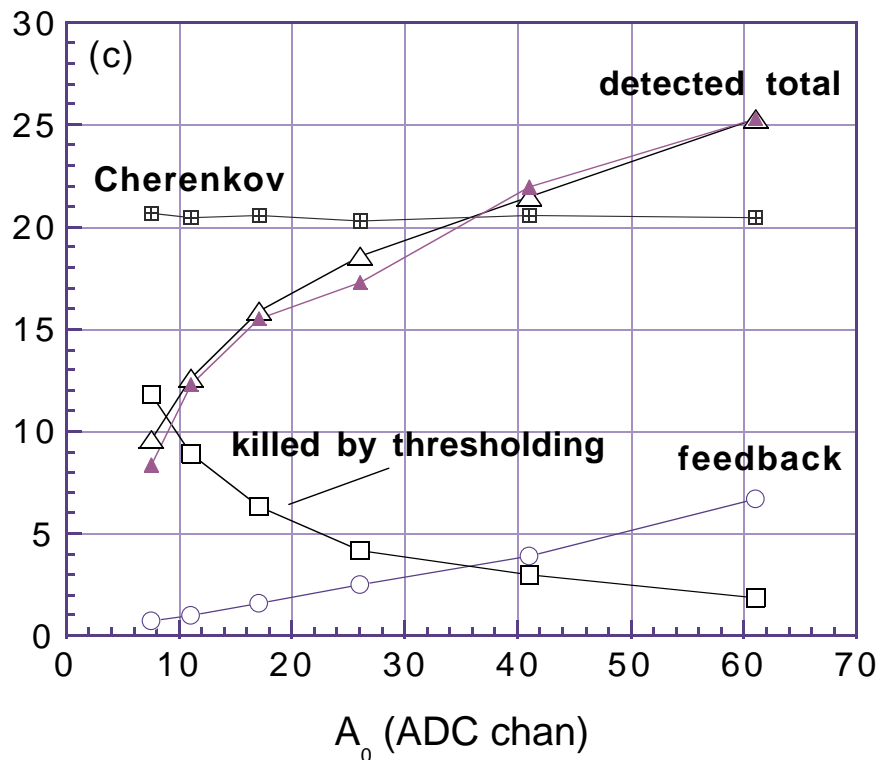
Feedback photons in CsI chambers



- could be dangerous: open geometry
- less problematic: thin gas volume

- **working point:** gas amplification is a compromise between **detection efficiency** and **cluster size and overlap, detector occupancy**.

RD-26 study: performance vs. gas amplification

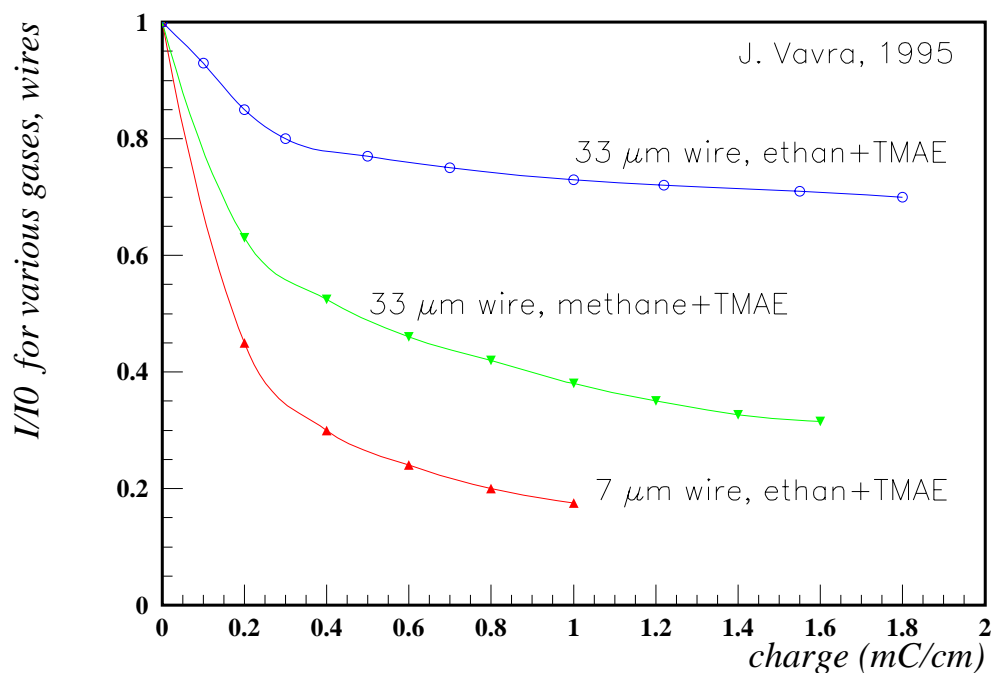


Number of detected photoelectrons vs. average pulse height

Anode wire ageing

Cause: accumulation of polymerisation deposits on the anode wires, particularly in TMAE loaded gases.

Consequence: gas amplification drops as a function of deposited charge.



— > J. Vavra et al., NIM **A367** (1995) 353-357.

Note again that the single electron detection efficiency depends exponentially on the average pulse height, and thus on the amplification,

$$\epsilon = e^{-\frac{U_{th}}{U}}$$

for the pulse height threshold set to U_{th} .

A drop of amplification by a factor k decreases the efficiency to

$$\epsilon' = e^{-\frac{U_{th}}{U/k}} = \epsilon^k,$$

e.g. if we start with a 90% single electron detection efficiency, a drop of amplification by a factor of 6 reduces the efficiency to about 50%, while starting at 80% we arrive at 50% already after a drop of factor 3 in amplification.

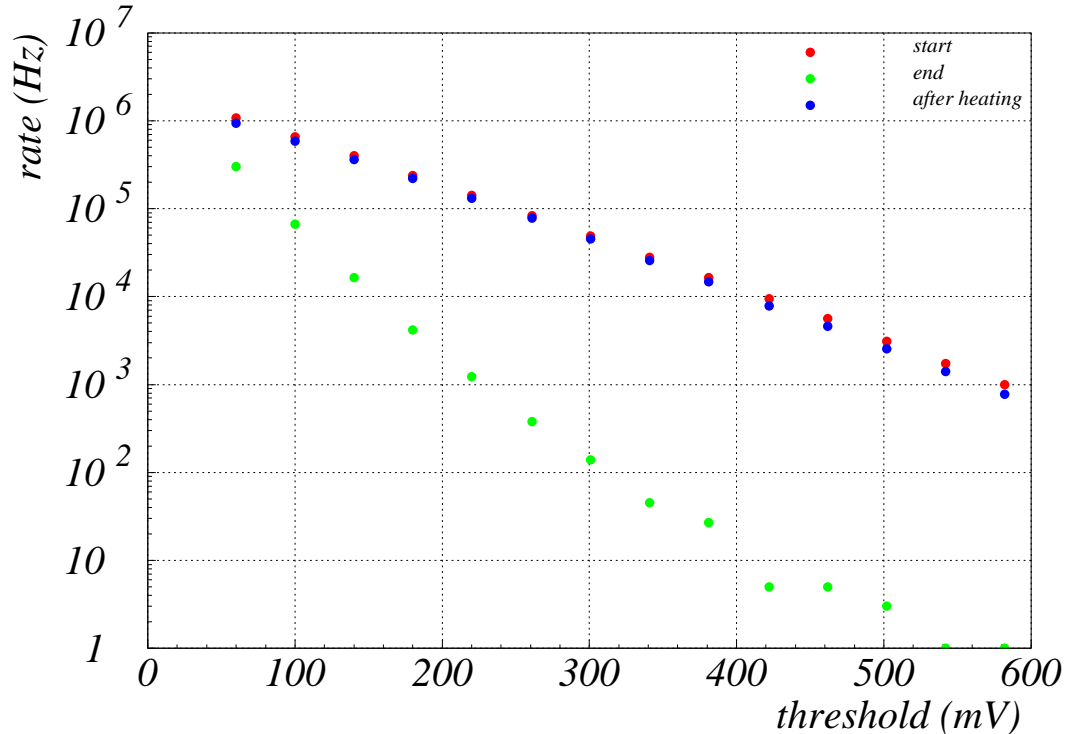
Recovery?

The initial performance can at least in principle be restored if the high voltage is increased (a rise by 200V increases the gas amplification by about a factor of 2.4 in a methane filled chamber with $20\mu m$ anode wires), but this clearly cannot be carried out too many times if we already start with an operating voltage of 2400V, in particular for cases where the irradiation is not uniform over the chamber.

Deposits can be removed by **washing** the wires **with alcohols**, or **heating** the wires (**attractive because one can do it in situ**).

SLD CRID pioneered this technique by using **carbon** wires (high resistivity). — > J. Va' vra et al., IEEE Trans. Nucl. Sci. 45 (1998) 648-656.

Example of the performance of a *in situ* heatable anode wires for high rate applications



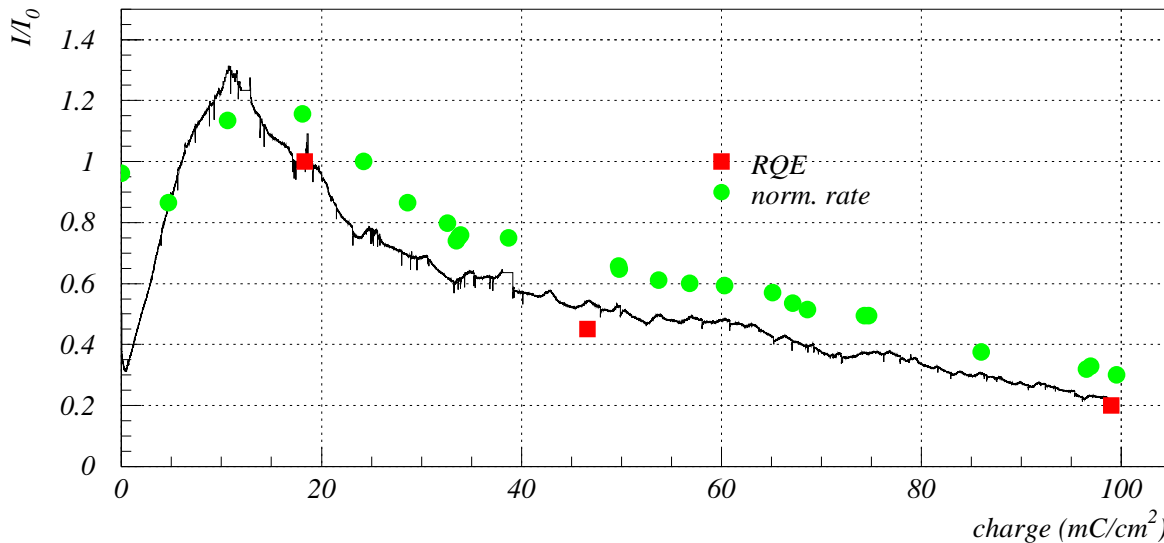
Threshold scan **before the irradiation**, **after** the irradiation, and **after the heating** - HERA-B prototype. — > see poster D. Škrk et al., NS20-57, NSS Posters I, for details

Cathode related effects

- TMAE: Accumulation of polymerisation deposits on the cathode planes (typically good insulators) can cause a large electric field after enough charge has accumulated, making possible the emission of electrons from the cathode - [Malter effect](#). This, in turn, can cause periodic bursts of charge - observed in the SLD CRID – > J. Va'vra, NIM A367 (1995) 353-357.

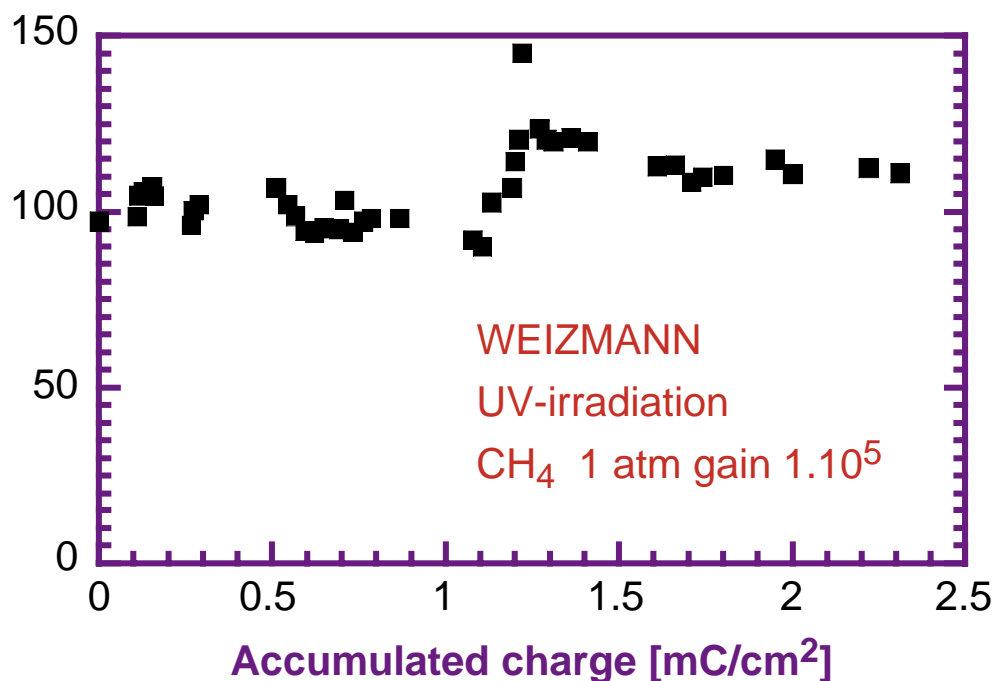
[Remedy?](#) As a possibility adding water (at tens of ppm level) was proposed, with the idea that it would help in the same way it does in drift chambers, i.e. make the cathode more conductive.

- **CsI: Photocathode ageing:** decay of the CsI layer during the recombination of ions from the avalanches.



An example of CsI ageing: after an initial sharp decay (from 1. to 0.3), the photocathode recovers, and then starts gradually losing q.e.

CsI ageing: less pronounced at lower rates?



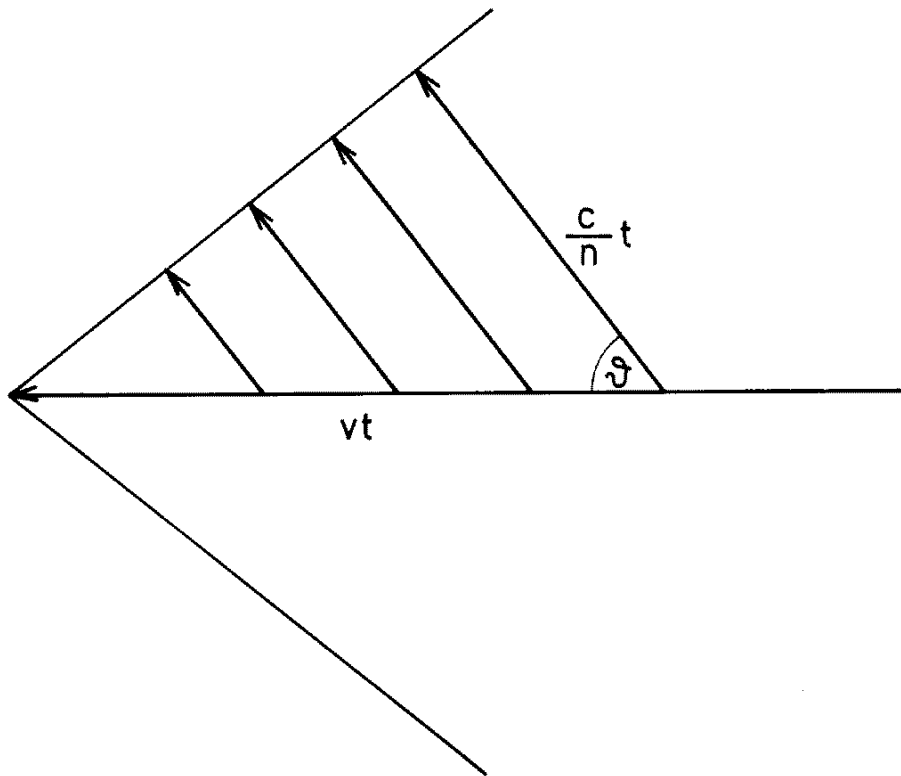
Ageing effects were also reported at high photon fluxes even without gas amplification.

Remedy? Protective covers were tried - little success.

-> Make the chamber in such a way that the photo-cathode (backplane of the chamber) can be easily exchanged.

Čerenkov effect

A charged track with a velocity above the speed of light in the medium with the index of refraction n emits light at a characteristic angle.



Speed of light: $\frac{c}{n}$, c : speed of light in the vacuum

Track velocity: $v = \beta c$

Čerenkov angle

$$\cos \vartheta = \frac{c/n}{v} = \frac{1}{\beta n}$$

The number of Čerenkov photons emitted over unit length and photon energy

$$\frac{d^2 N}{dx dE} = \frac{\alpha}{\hbar c} \sin^2 \vartheta$$

where $\frac{\alpha}{\hbar c} = 370 \text{ eV}^{-1} \text{ cm}^{-1}$

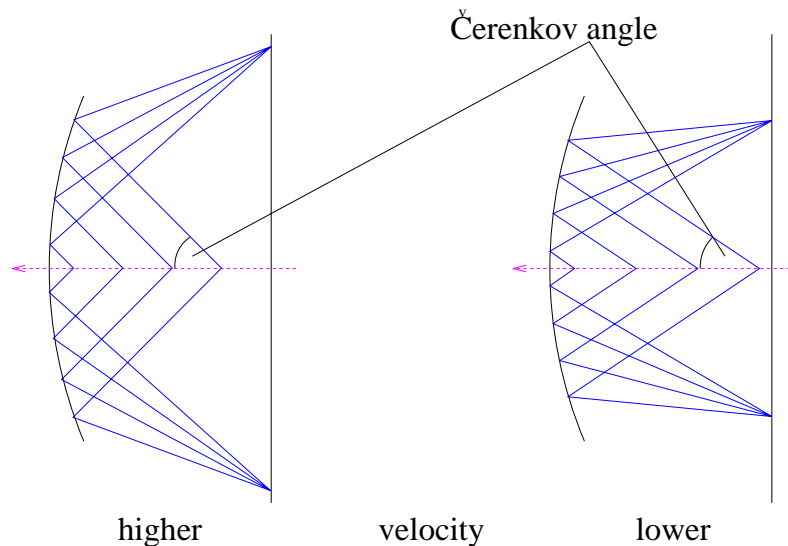
Example: in 1 cm of water ($n = 1.33$) a track with $\beta = 1$ emits $N = 320$ photons in the spectral range of visible light ($\Delta E \approx 2 \text{ eV}$). If Čerenkov photons were detected with an average detection efficiency of $\epsilon = 0.1$ over this interval, $N = 32$ photons would be measured in the above example.

RICH counter

Aim: measure the direction of Čerenkov photons emitted by a charged track

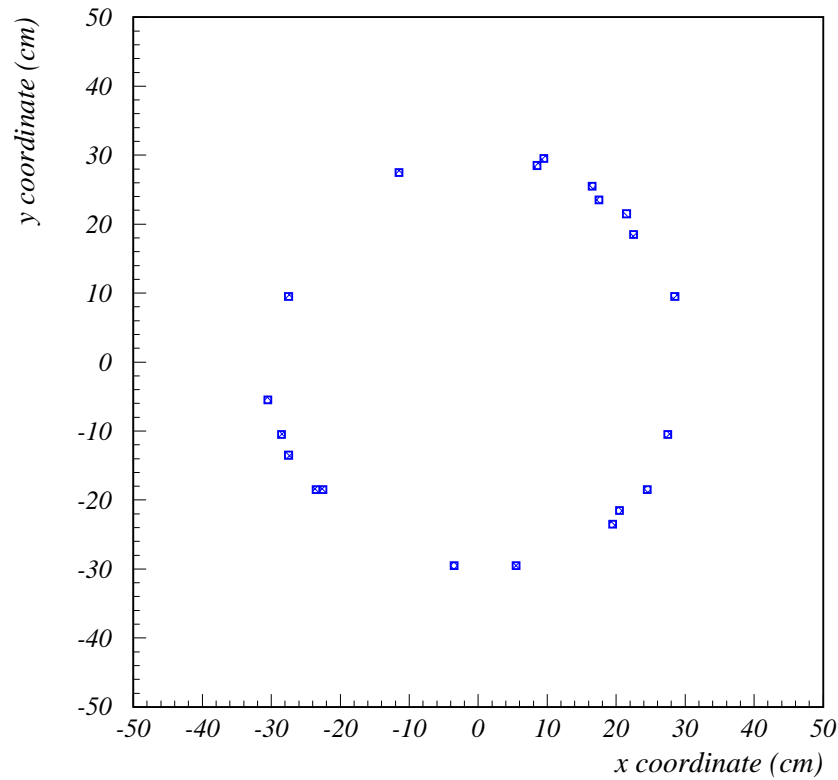
Idea: transform the **direction** into a **coordinate**.

Take a **spherical mirror**: parallel rays intersect on the focal surface.

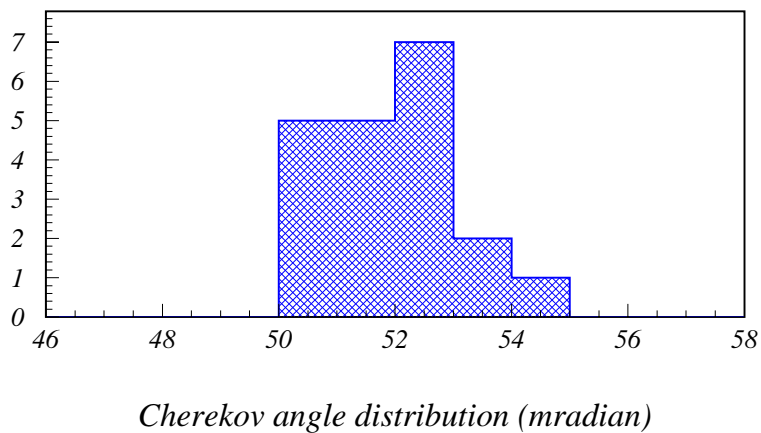


Since photons are emitted uniformly over the azimuthal angle around the track, a ring is formed on the focal plane.

With a **position sensitive photon detector** on the focal plane we arrive at a **Ring Imaging Čerenkov counter (RICH)**



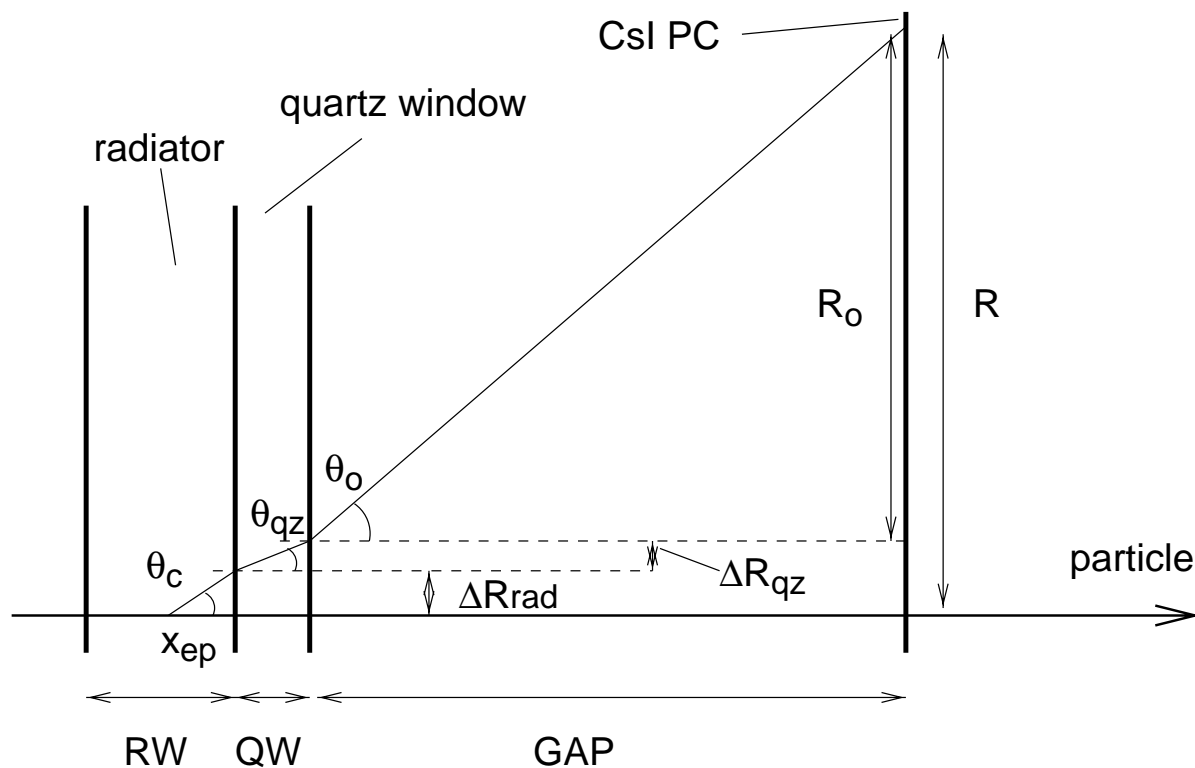
From the picture on the photon detector, the Čerenkov angle of the track can be reconstructed, i.e. from the known track direction (ring center) and hit coordinate the angle is calculated and plotted:



Proximity focusing RICH

Geometry variation: in case of a solid or liquid radiator, the radiator thickness is only about 1 cm - one does not need a spherical mirror.

Photons are let to propagate over a distance of 10-20 cm, until they reach the photon detector.



Photosensitive material - chamber combinations

TEA • multiwire chamber with pad read-out (College de France, CLEO III)

TMAE • TPC (Omega, DELPHI, SLD)

- multiwire chamber with pad read-out (Caprice)
- two parallel plate stages, coupled to a multiwire chamber with pad read-out (CERES)

CsI • multiwire chamber with pad read-out (College de France/CERN, RD26 - CERN, RD26 - Saclay, HADES prototype (TU Munich), HERA-B prototype, Princeton, Compass prototype)

- MSGC and MGC (HADES prototype, Weizmann, Pisa) with a transmissive photocathode
- chamber with a GEM preamplification stage (Weizmann)

Resolution of a RICH counter

Sources of error in the velocity determination,

$$\beta = (n \cos \theta)^{-1},$$

if measured by a single photon are (example: HERA-B geometry, TMAE-methane chambers, C₄F₁₀ radiator gas):

- The finite coordinate resolution of the photon detector

$$\begin{aligned}\sigma_{\beta}^{det} &= n \sin \theta \sigma_{\theta} = \\ &= \sqrt{2(n-1)} \frac{a}{f \sqrt{12}} = 2.02 \cdot 10^{-5},\end{aligned}\quad (1)$$

with a pad size of $a = 7.5$ mm and a focal length of $f = 6$ m.

- Dispersion, variation of the refractive index over the energy range of those Čerenkov photons that are seen by the photon detector. With $(dn/dE) = 5.3 \cdot 10^{-5} \text{ (eV)}^{-1}$ and the RMS $\sigma_E = 0.4$ eV, this amounts to

$$\sigma_{\beta}^{dis} = \frac{dn}{dE} \sigma_E = 2.15 \cdot 10^{-5}, \quad (2)$$

- plus the optical error due to the imperfections on the mirror surface and mirror misalignment, the error due to the finite precision in track slope parameters as determined by the tracking system, the optical error due to the nonzero angle of incidence of photons upon the spherical mirror (spherical aberration), (all expected to be considerably below the first two)

The combined single photon error for high momentum tracks amounts to

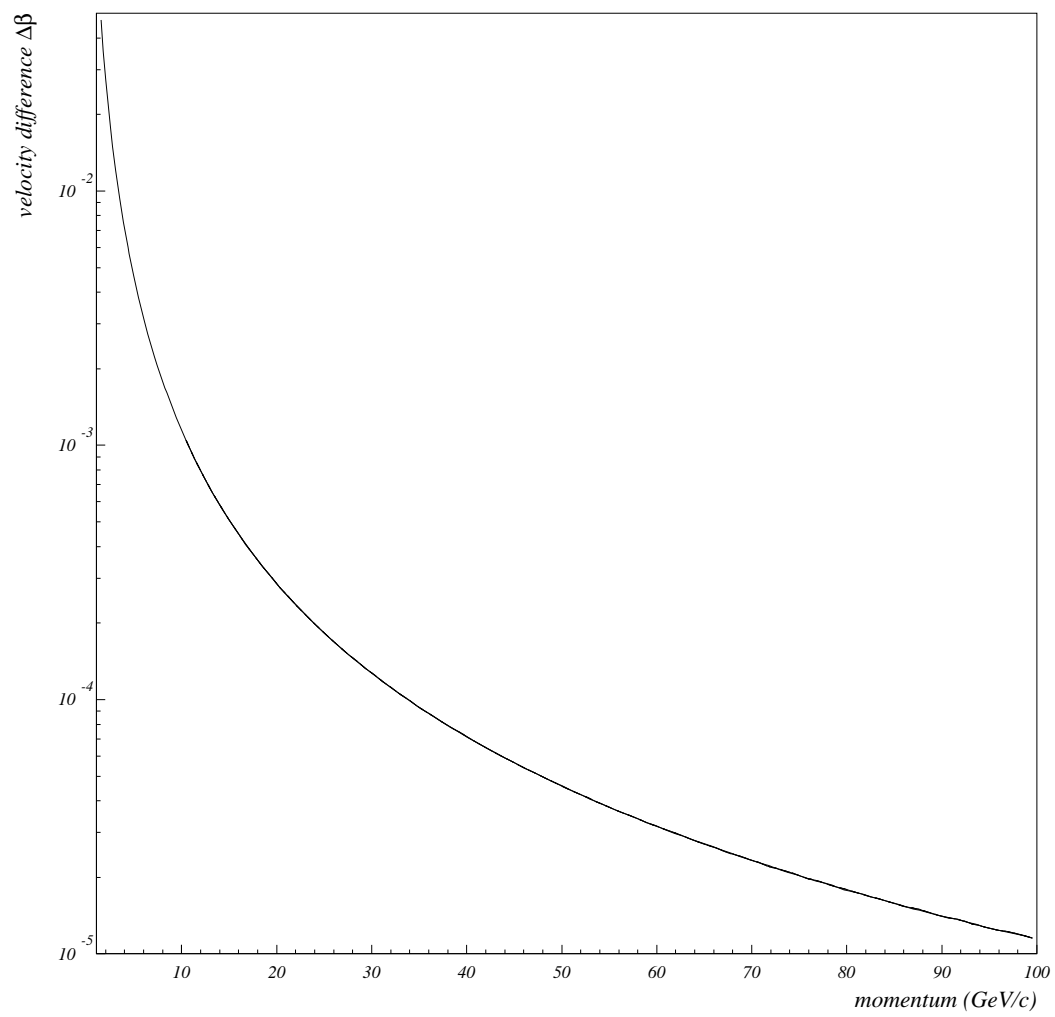
$$\sigma_{\beta} = 3.31 \cdot 10^{-5} , \quad (3)$$

corresponding to a resolution in Čerenkov angle of 0.59 mrad.

Assuming 25 detected photons for a $\beta = 1$ particle, the measurement precision is

$$\sigma_{\beta}^{(N)} = \frac{\sigma_{\beta}}{\sqrt{N}} = 0.66 \cdot 10^{-5} . \quad (4)$$

In absence of backgrounds, the proposed counter would thus enable a 3σ pion-kaon separation up to 70 GeV/c for isolated tracks.



Velocity difference for pions and kaons.

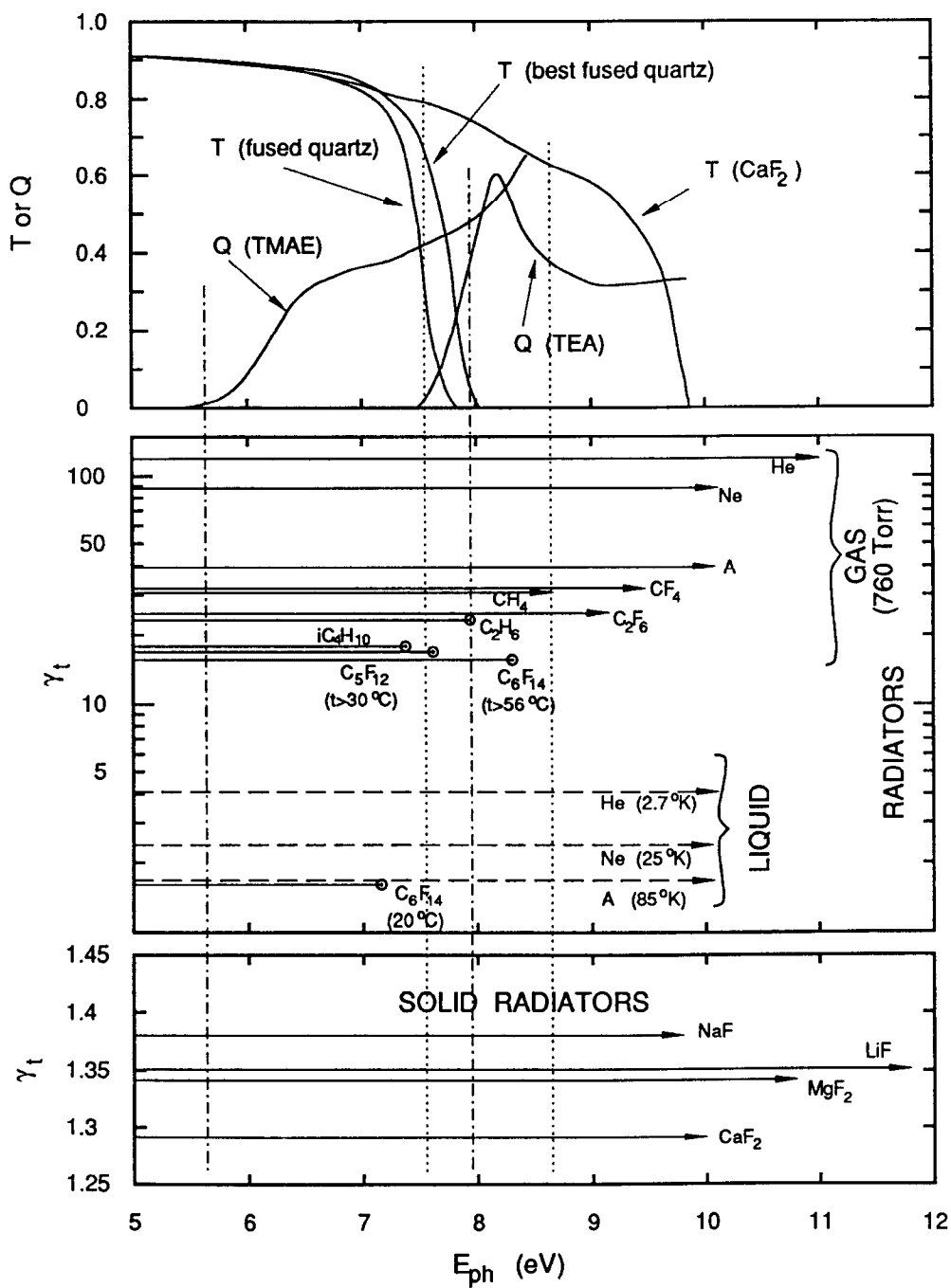
Radiator choice

The choice of RICH radiator medium in case of a specific experiment depends on the particles we would like to identify, and their kinematics:

- the threshold momentum for the lighter of the two particles we want to separate $p_t = \beta_t \gamma_t m c$, $\beta_t = 1/n$ roughly coincides with the lower limit of momentum spectrum
- the resolution in Čerenkov angle has to allow for a separation up to the upper limits of kinematically allowed momenta, while of course
- radiator has to be transparent for the wavelengths the photon detectors can see.

Irreducible contribution to finite resolution: dispersion.

Variation in n over the interval 6.5 eV - 7.5 eV (TMAE/CsI region): dn/dE in units 10^{-5} eV^{-1} : gases CF_4 2, argon 2.1, methane 4.9, C_4F_{10} 5.3, isobutane 16, liquid C_6F_{12} 930



Detection efficiency/radiator transmission windows.

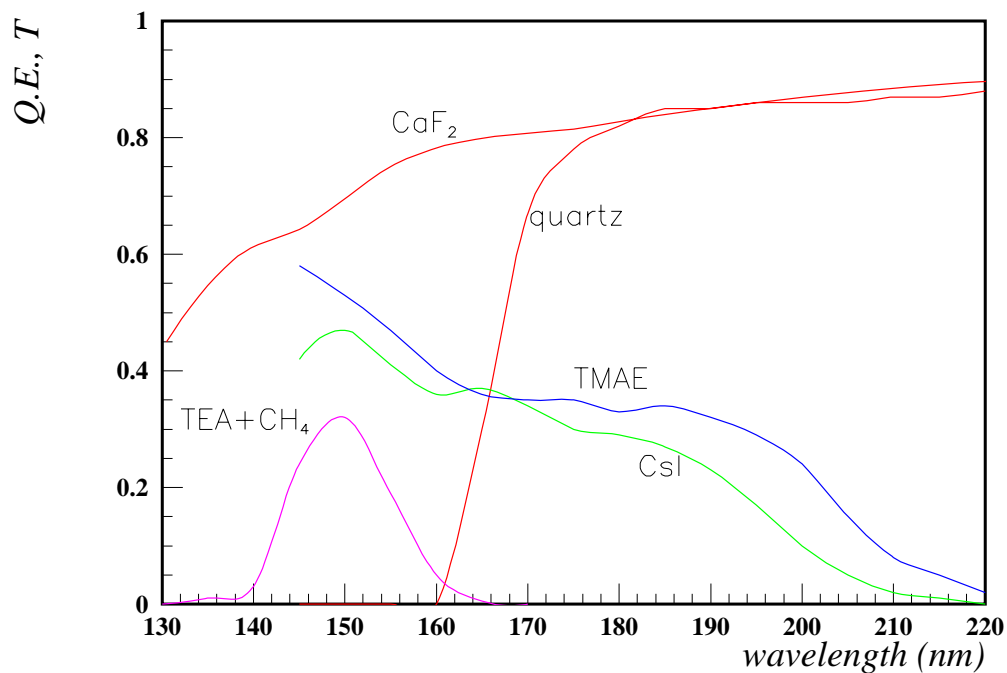
Chamber windows

Transmission of chamber windows has to match the photosensitive substance.

quartz for TMAE, CsI

CaF₂ for TEA

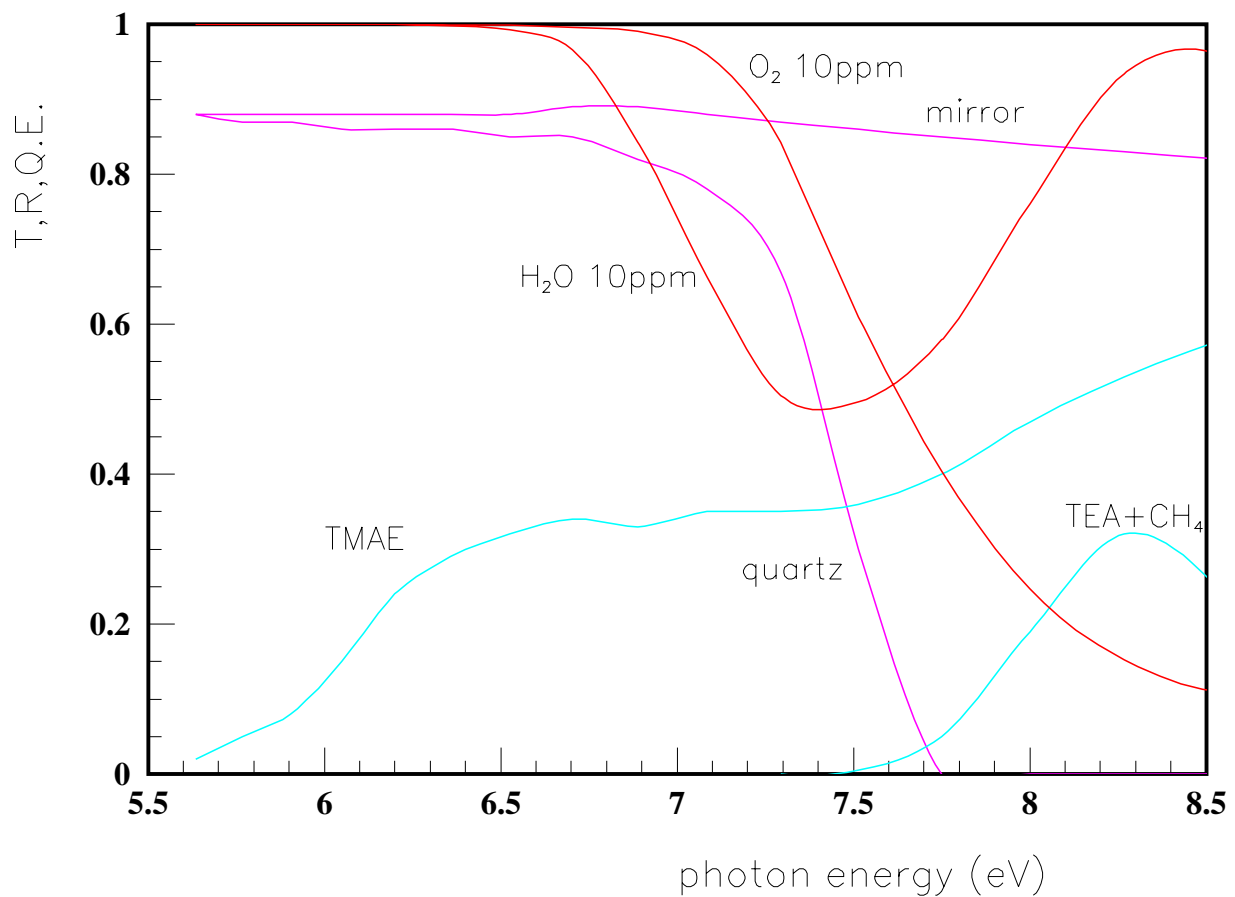
For comparison: mylar is only transparent above ≈ 400 nm, UVT plexiglass above 300 nm.



Large systems

Water and oxygen content in the radiator (order meter to few meters of gas, or centimeter of liquid) have to be kept very low.

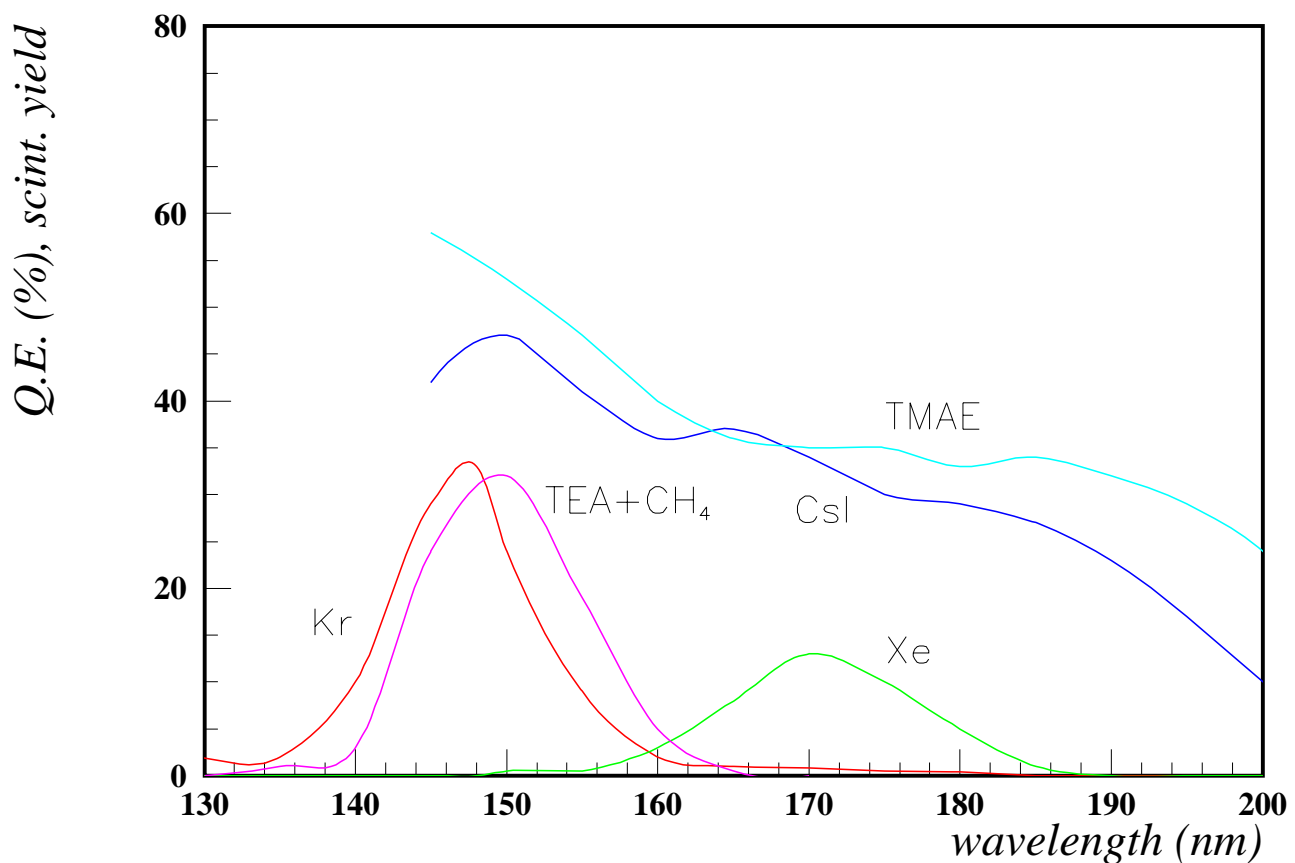
Example HERA-B: average photon path is 7.5 m.



Other applications of light sensitive wire chambers

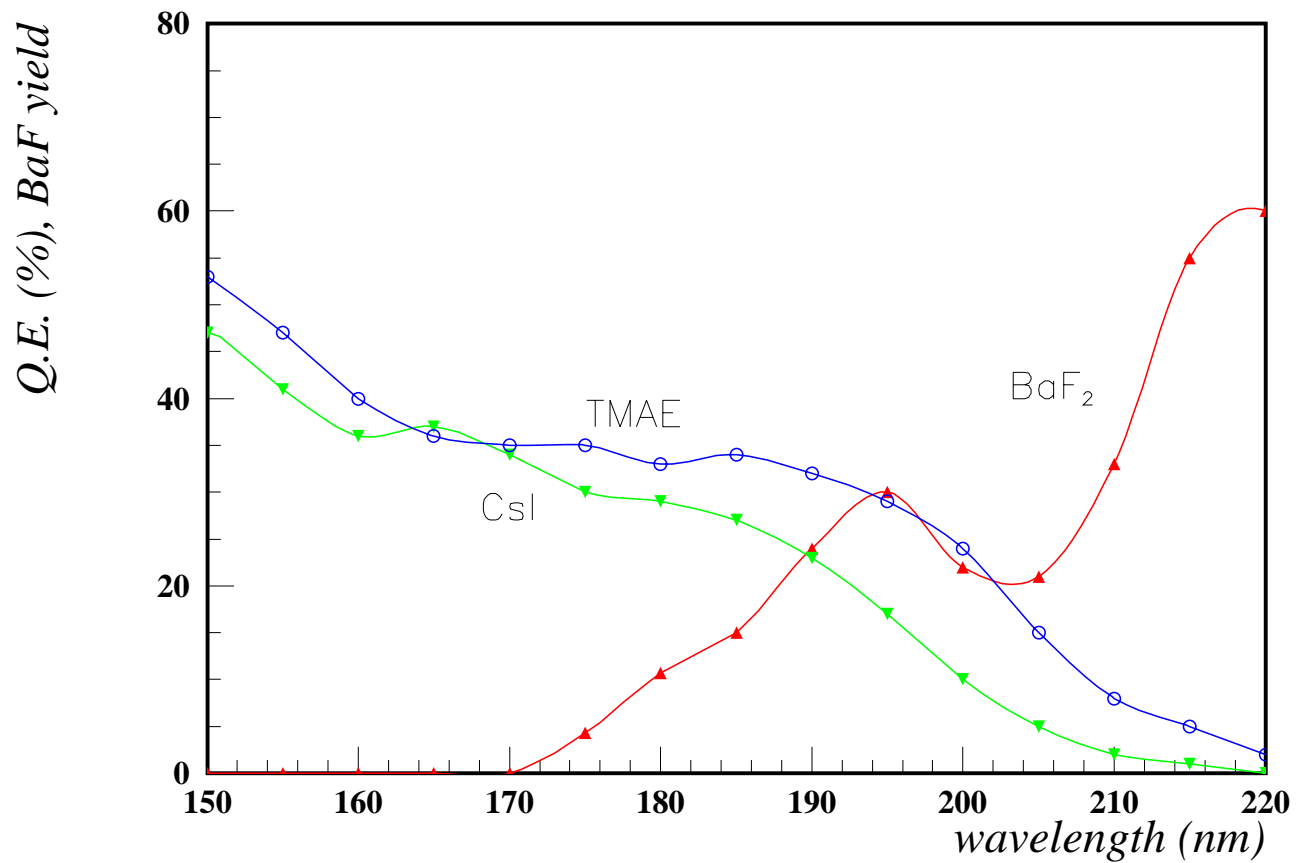
UV light sensitive wire chambers can be coupled to:

- gas scintillation proportional chambers: read-out of scintillations in noble gases



-> better X-ray energy resolution than direct detection via photoeffect in gas

- solid scintillators: read-out of the fast component of BaF_2



-> a fast position sensitive detector of γ rays, e.g.
for PET applications

Summary

- Detection of UV photons is not trivial.
- However: large system have been successfully operated for years.
- A new generation of experiments is under design/contruction.
- Visual photon detection: being developed.
- High rate operation: problematic, in particular if long term stability is required - more R+D needed to become competitive with PMTs.

More on the subject:

1. UV photon detection: overviews

- J. Va'vra, Photon detectors, NIM **A371** (1996) 33-56.
- A. Breskin, CsI UV photocathodes: history and mystery, NIM **A371** (1996) 116-136.
- F. Piuz et al., ALICE HMPID, CERN/LHCC 98-19.

2. avalanche development, pulse height statistics

- P. Rice-Evans, Spark, streamer, proportional and drift chambers, Richelieu, London (1974)
- F. Sauli, Principles of operation of multiwire proportional and drift chambers, in Experimental techniques in High-Energy Nuclear and Particle Physics, T. Ferbel (editor), World Scientific (1991)

3. Čerenkov counters: overview

- J. Seguinot and T. Ypsilantis, A historical survey of ring imaging Čerenkov counters, NIM **A343** (1996) 1-29.
- T. Ypsilantis and J. Seguinot, Theory of ring imaging Čerenkov counters, NIM **A343** (1996) 30-51.

4. Čerenkov counters: status

- Proceedings of the First Workshop on Ring Imaging Čerenkov Detectors - Experimental Techniques of Čerenkov Light Imaging, Bari, Italy, June 2-5, 1993, NIM **A343** (1996).
- Proceedings of RICH '95: International Workshop on RICH Counters, Uppsala, Sweden, June 12 - 16, 1995, NIM **A371** (1996).
- Proceedings of RICH '98: Ein Gedi, Israel, Nov. 15 - 21, 1998, to be published as a volume in NIM A.